Octanol-Triggered Self-Assemblies of the CTAB/KBr System: A Microstructural Study

Lisa Sreejith,*[,†] Sudheesh Parathakkat,[†] Sreejith Muraleedharan Nair,[‡] Sanjeev Kumar,[§] Gunjan Varma,[∥] Puthusseril A. Hassan,[∥] and Yeshayahu Talmon[⊥]

Soft Materials Research Laboratory, Department of Chemistry, National Institute of Technology, Calicut, India, PG and Research Department of Chemistry, Malabar Christian College, Calicut, India, Department of Chemistry, The Maharaja Sayajirao University of Baroda, Vadodara, India, Chemistry Division, Bhabha Atomic Research Centre, Trombay, India, and Department of Chemical Engineering, Technion-Israel Institute of Technology, Haifa, Israel

Received: May 12, 2010; Revised Manuscript Received: September 24, 2010

A micelle−vesicle transition induced by *n*-octanol C_8OH was observed in an aqueous cetyltrimethylammonium bromide (CTAB)/potassium bromide (KBr) system. This transition was investigated by viscosity, rheology, dynamic light scattering (DLS), and direct imaging technique, cryo-transmission electron microscopy (cryo-TEM). Viscometry shows that the system underwent several morphological transitions with the increase in concentration of C_8OH (regions I−IV). At low octanol concentration (region I), DLS analysis showed an increase in the apparent hydrodynamic diameter of the micelles with the addition of C_8OH which was supported by cryo-TEM and rheology. With further addition of C_8OH, transition of the elongated micelles occurred to a viscoelastic fluid comprising entangled wormlike micelles (region II), for which rheological data can be described by the Maxwell model. Further, the wormlike micelles transform to vesicles at $[C_8OH] \approx 0.020$ M (region III). This transition and the consequent changes in the fluid response can be explained in terms of vesicle formation caused by further addition of C_8OH. Beyond this concentration (region IV), vesicles are the predominant microstructures in the system which shows unusual temperature response.

Introduction

Surfactant molecules self-assemble into different microstructures in aqueous solution, like micelles, vesicles, and the lamellar phase depending on the solution composition, and are shown to have a strong influence on the rheological properties of the fluid.[1−5] An increase in surfactant concentration, change in temperature or pH, and the addition of cosurfactant, salt, or an oppositely charged surfactant can promote micelle growth. In certain cases, the spherical micelles can grow anisotropically leading to highly viscous solutions consisting of flexible wormlike micelles. Wormlike micelles were found to entangle with each other to form a transient network above some critical concentration, called the overlap concentration, and thus exhibit viscoelastic properties.[6,7] The wormlike micelles break and recombine in a characteristic time scale depending on the prevailing physicochemical conditions and therefore exist in a dynamic equilibrium,[8] referred to sometimes as "living polymers". They may, therefore, function as reversible thickening and rheology control agents in aqueous formulations, in a way similar to high molecular weight polymers. It is well-known that salts like KBr and NaSal induce pronounced growth of cationic micelles due to screening of the electrostatic repulsion of head groups.[9,10] The size and shape of the micelle are influenced by the counterion distribution or condensation on the micelle surface.[11] The effect of KBr on the microstructure of cetyltrimethylammonium bromide (CTAB) micelles has been investigated by Weican et al.,[12] and they showed that the hydrodynamic radius, R_h, of the CTAB micelles (0.01 M) increased from 3.5 to 43 nm with the addition of 0.6 M KBr. Here, the molecular weight of micelles is also found to increase appreciably. Among the micelle structures, viscoelastic wormlike micelles have attracted much interest in fundamental research and practical applications. The microstructure of wormlike micelles is correlated to a packing parameter, R_p, of approximately 1/2. The effective headgroup area (a_h) is affected by an additive in the solution and is responsible for increased R_p and, therefore, transition to higher-order aggregates, e.g., wormlike micelles.[13] Such wormlike micelles increase the viscosity of fluids like polymer.

The effect of aliphatic alcohols on the size and shape of the micelles has also been reported.[14−16] Medium chain length alcohols (C_4−C_7OH, where C is the carbon number present in the alkyl chain) partition themselves to the micelles and to the background solution. The micelle-bound alcohol intercalates between the surfactant ionic head groups and decreases the micelle surface charge density. The addition of long-chain alcohols (C_8OH and above) increases the aggregation number producing mixed micelles.[17,18] Kumar et al.[19] and Desai et al.[20] studied the micelle growth of cationic micelle systems in the presence of alcohols and amines and found that C_8OH is more effective in promoting the sphere-to-rod transitions. The zero shear viscosity of these solutions showed peak behavior, and the peak shifts to lower [additive] with increasing content of surfactant or salt in the system. The increase in viscosity is attributed to the formation of wormlike micelle networks, and the decrease is due to the decrease in the mean size of the network or due to the formation of other morphologies, e.g., vesicles.[21,22] Vesicles are aggregates of surfactant bilayers bent in the form of concentric spheres entrapping large volumes of

* Corresponding author. Tel.: +91-495-2286553. Fax: +91-495-22867280. E-mail: lisa@nitc.ac.in /drlisasreejith@gmail.com.
† National Institute of Technology, Calicut.
‡ Malabar Christian College.
§ The Maharaja Sayajirao University of Baroda.
∥ Bhabha Atomic Research Centre.
⊥ Technion-Israel Institute of Technology.

10.1021/jp1043255
Published on Web 12/30/2010

water that find a variety of applications in the food industry, cosmetics, drug delivery, etc.[23−25]

The association structure can be molecularly simulated.[26] Surfactant microstructures continue to attract widespread industrial and scientific attention ranging from applications in detergent formulations to self-assembly of protocells and controlled drug delivery.[2] Control of surfactant self-assembly using additives is critical in many of these applications and could provide a breakthrough in the construction of artificial biomimetic architectures.[27] Several surfactant systems in which a change in aggregate morphology is triggered by additives have been reported.[28−30] However, systems in which the on/off assembly and disassembly of amphiphiles can be triggered remain largely unexplored.

In our earlier studies, we have reported, for the first time, the formation of a gel phase[31] with a Maxwell behavior,[32] when C_8OH and KBr are simultaneously added to aqueous CTAB. This can be ascribed to the formation of shear-induced structure which is sensitive to concentrations of cosurfactant. Several studies are performed on similar surfactant systems, but detailed microstructural characterization of aggregates has not been explored much.[14−20] Micelle to vesicle transition (MVT) with increasing [additive] has been described in the past for a couple of systems to our knowledge.[7,28] The viscosity increase with temperature is another important observation which is reported only for a few other surfactant systems.[28,33] Keeping this view in mind, we have undertaken a detailed study of the microstructures present in the aqueous surfactant/additive system (CTAB + KBr + C_8OH) using viscometry, rheology, dynamic light scattering (DLS), and cryo-TEM. Viscometry facilitates determination of various concentration ranges of C_8OH under which different morphologies coexist. Rheology and DLS support the viscometry data, while cryo-TEM provides direct visualization of the aggregates proposed in the initial part of the study. MVT is an advantageous method for loading substances and a critical step in reconstituting membrane proteins into vesicle membranes that provide a biomimetic environment. The simplicity and ease of preparation of the present system might make it attractive for various applications mentioned above.

Experimental Methods

The micellar solutions of 0.1 M CTAB (BDH, England, 99% assay) with 0.1 M KBr (Ellis Dugal, India, 99% assay) and *n*-C_8OH (Merck, Germany, 99% assay) were prepared in deionized Milli-Q water and kept in a water bath at a temperature of 45 °C with shaking for about one hour for homogeneity. The samples were then cooled and kept at room temperature for at least two days to attain equilibrium. Prior to the measurements, the samples were thermostatted at the measuring temperature for about 30 min. The rheological characterizations were carried out using a controlled stress rheometer (Anton Paar Physica MCR- 51) with a cone and plate sensor (40 mm diameter, 3.988° angle) at different temperatures. The viscosity profiles of the samples were acquired by varying the shear rate from 0.3 to 500 s^{-1}. Frequency sweep measurements were carried out by varying the angular frequency from 0.06 to 100 rad·s^{-1}. The experiments were performed at 1% strain within the linear viscoelastic range.

Dynamic light scattering (DLS) measurements were performed using a Malvern 4800 Autosizer employing a 7132 digital correlator. The light source was Ar-ion laser operated at 514.5 nm with a maximum power output of 2 W. The samples of micelle solutions were filtered through 0.2 mm filters (Millipore) to avoid interference from dust particles. Measurements were made at five different angles ranging from 50 to 130°. The measured intensity correlation functions were analyzed by the method of cumulants[33] where unimodal distribution of relaxation time is considered. The size distribution is obtained using the CONTIN algorithm wherever needed.

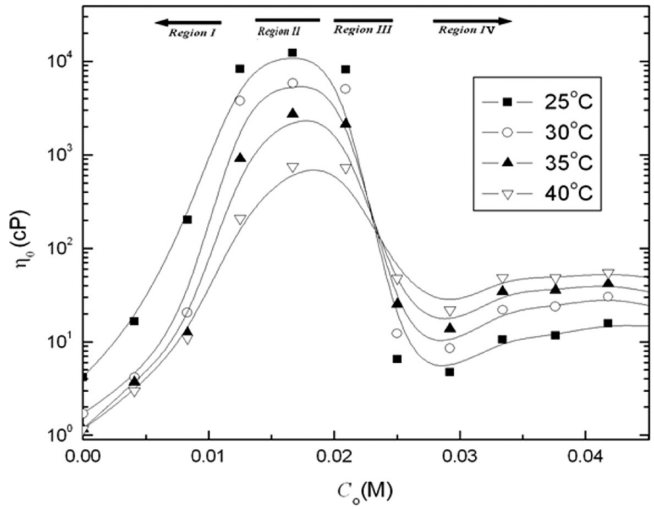

Figure 1. Effect of C_8OH concentration on the zero-shear viscosity η_0 (cP) of 0.1 M CTAB/0.1 M KBr micellar solutions at different temperatures.

Vitrified cryo-TEM specimens were prepared in a controlled environment vitrification system (CEVS),[34] at 25 °C and 100% relative humidity to avoid loss of volatiles, followed by quenching into liquid ethane at its freezing point. The specimens, kept below −178 °C, were examined by an FEI T12 G2 transmission electron microscope, operated at 120 KV, using a Gatan 626 cryo-holder system. Images were recorded digitally on a Gatan US1000 high-resolution cooled-CCD camera using the Digital Micrograph 3.4 software package in the low dose imaging mode.

Results and Discussion

Figure 1 shows the variation of zero shear viscosity (η_0) of aqueous 0.1 M CTAB/0.1 M KBr micelle solution upon addition of C_8OH in the temperature range 25−40 °C. It is observed that η_0 is a strong function of concentration of C_8OH (C_o) and is found to vary by several orders of magnitude. On the basis of the changes in viscosity of the solution, four different regimes have been identified: a steep rise in viscosity (region I), followed by a region of maximum viscosity, $\eta_0 \sim 10^4$ cp, (region II), a sharp decrease (region III), and then to a slow increase (region IV). At low C_o, initially present spherical (or ellipsoidal) micelles grow gradually with a concomitant increase in viscosity. A Coulombic interaction favors micelles with a higher surface area per head group. On the other hand, hydrophobic interaction between the hydrocarbon part of the micelles/monomers tries to achieve aggregates with closely packed monomer chains.

In region I, viscosity rises gradually in the initial part, while it increases steeply in the later half of the region. Moreover, viscosity levels off in region II. The wormlike micelles grow in length by assuming various shapes. We can expect spherical micelles (ellipsoidal micelles) or short rods in the initial part of region I. However, the viscosity increase caused by short rod-shaped micelles—with an axial ratio of the long axis over the short axis smaller than 4—is not very different from that due to spherical micelles.[36] Therefore, viscosity cannot be used

to establish the morphologies in each region. Hence, viscosity data shown in Figure 1 have been used to qualitatively distinguish various regions (I−IV).

Mukerjee[37] had proposed that an additive which is surface active to a hydrocarbon−water interface will be mainly solubilized at the headgroup region and will promote micelle growth. Therefore, C_8OH is expected to be embedded between CTAB monomers of the micelles. This embedding of C_8OH may increase the volume of the micelle which is equivalent to an increase in the length of the surfactant monomer. These factors modify the effective surfactant packing parameter, R_p, and are responsible for the micelle growth and hence viscosity increase observed in region I (Figure 1). The result then is the trend: spherical micelle → rodlike (wormlike) with larger structures, with increasing [C_8OH]. When micelles are sufficiently long they convert more flexible wormlike micelles (in region II) which can flow comparatively easily, and hence a level off in the log η_0 vs [C_8OH] plot is observed. For hydrocarbon-based surfactants, it has been proposed[38] that the micellar structure is strongly influenced by R_p, and consequently, different microstructures are expected at higher [C_8OH]. A steep fall in η_0 (and appearance of turbidity) indicates a transition to a new morphology (region III). A decrease of nearly 3 orders of magnitude in η_0 and the appearance of the system are hinting to a vesicular phase. Similar behavior was observed in a few surfactant systems and was explained by the above reasoning.[28,39] At further higher concentrations of C_8OH, viscosity shows a slow increase, and the samples appear almost clear (region IV). If we compare the sample viscosity at each temperature (region IV), it can be seen that for the same system η_0 increases with temperature (an unusual behavior).[40]

The increase of viscosity (similar to that of region IV) was explained on the basis of conversion of vesicles to a rod-shaped micelle transition.[28,33] In region IV, it is expected that a sufficient amount of C_8OH will be present which will be embedded between the head groups. In this situation, if we increase the temperature, then the Br^- ion may be released and would show higher preference for the bulk phase. Such a release, if it occurs, would increase the effective headgroup area (a_h), thereby driving the vesicles to aggregates of higher curvature resulting in an increase in viscosity. This indeed was observed in region IV. It was observed in our earlier study that the system converts again to a fairly viscous fluid (gel-like) with a thermo-reversible response[31] at further high concentration of C_8OH. In the present study, a rich microstructural behavior exhibited in a simple and easily preparable sample is reported for the first time. In the following paragraphs, we would like to shed more light on probable microstructures present in each region. Thus, we have selected representative samples from our preliminary viscosity measurements.

Detailed rheology of the system (0.1 M CTAB/0.1 M KBr/x M C_8OH) showed Newtonian behavior (up to 0.008 M) over the entire shear rate, $\dot{\gamma}$, which indicates that at low [C_8OH] nearly spherical micelles (or small rods) are present. Above 0.008 M, the viscosity decreases drastically with an increase in shear rate (shear thinning behavior), an indication of the formation of rigid rods of medium length, which slowly converts to a flexible cylindrical micelle (wormlike micelle). These samples were viscoelastic in nature and exhibited flow birefringence, which are characteristics of wormlike micelles.[28] The viscoelastic properties of the samples were analyzed by oscillatory-shear experiments (Figure 2), and at low frequencies the behavior can be described according to the Maxwell model.[41,42]

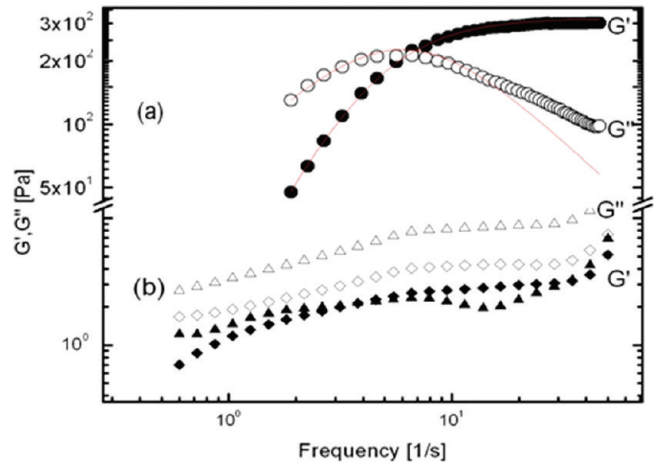

Figure 2. Variation of elastic modulus, G' (Closed), and viscous modulus, G'' (Open), with oscillation frequency (ω), for the 0.1 M CTAB + 0.1 M KBr + x M octanol micellar system of different [octanol] at 30 °C: (a) wormlike micelles and (b) vesicle phase. The bold line in the figure is indicative of the Maxwell fit.

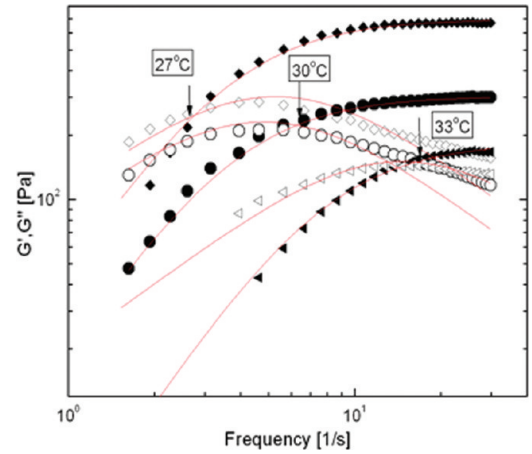

Figure 3. Variation of elastic modulus G' (closed symbols) and viscous modulus G'' (open symbols) with oscillation frequency (ω), for 0.1 M CTAB/0.1 M KBr/0.016 M octanol micellar system at three different temperatures. The solid lines represent the best fit to the Maxwell model.

For a Maxwell fluid, the variation of the elastic modulus G' and viscous modulus G'' can be given as

$$G'(\omega) = \frac{\omega^2\tau^2}{1 + (\omega\tau)^2}G_0 \quad (1)$$

$$G''(\omega) = \frac{\omega\tau}{1 + (\omega\tau)^2}G_0 \quad (2)$$

The complex viscosity η^* can be given as[31,32]

$$|\eta^*| = \frac{(G' + G'')^{1/2}}{\omega} = \frac{\eta_0}{\sqrt{1 + \omega^2\tau^2}} \quad (3)$$

For the viscoelastic system following Maxwellian behavior, η_0 values were estimated from the following equation.

$$\eta_0 = G_0\tau \quad (4)$$

where G_0 is the shear modulus.

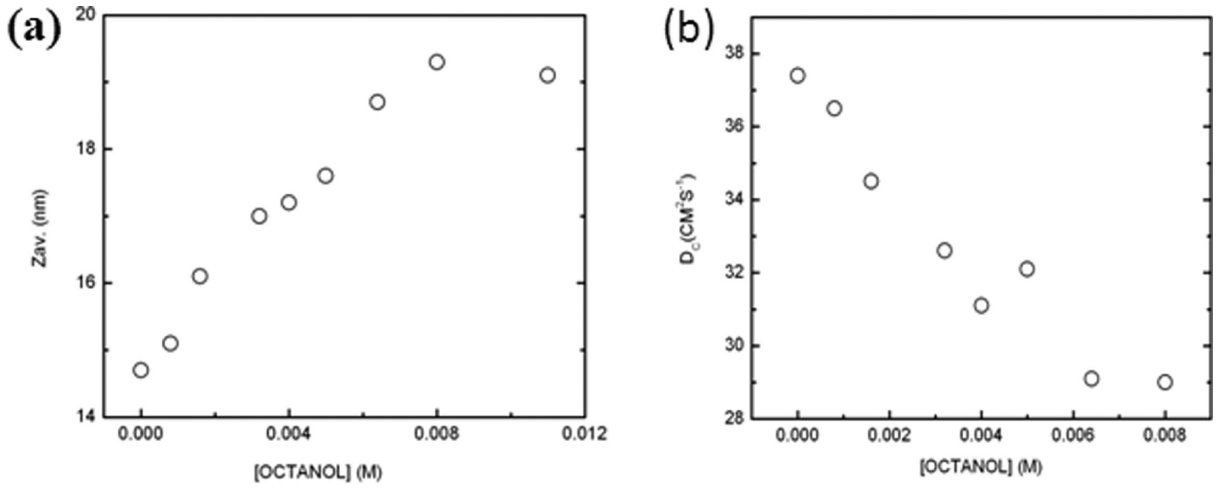

Figure 4. Variation of z-averaged apparent diameter (a) and apparent diffusion coefficient (b) of the micellar phase as a function of [C_8OH] in 0.1 M CTAB/0.1 MKBr solution.

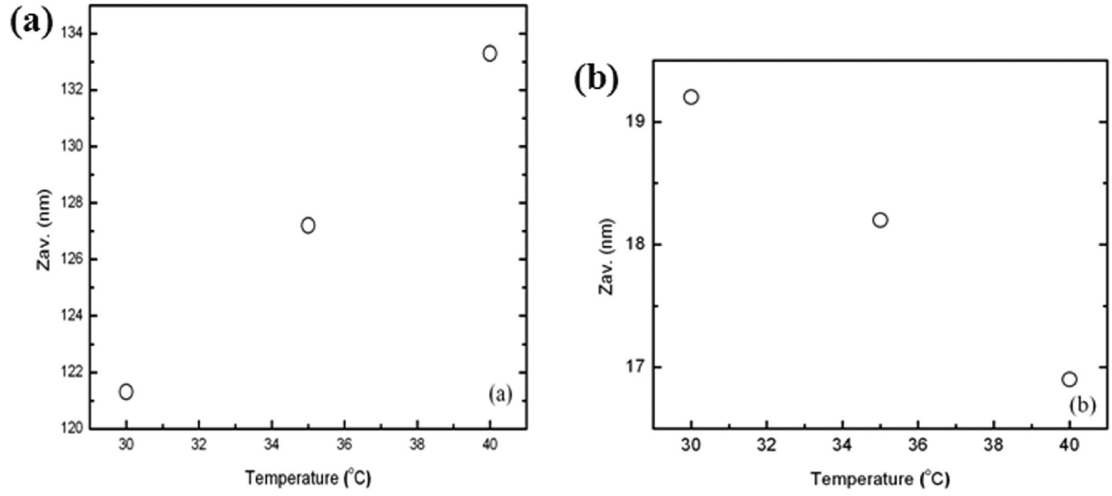

Figure 5. Variation of z-averaged apparent diameter of the 0.1 M CTAB/0.1 M KBr/octanol vesicle phase (a) and micellar phase (b) as a function of temperature.

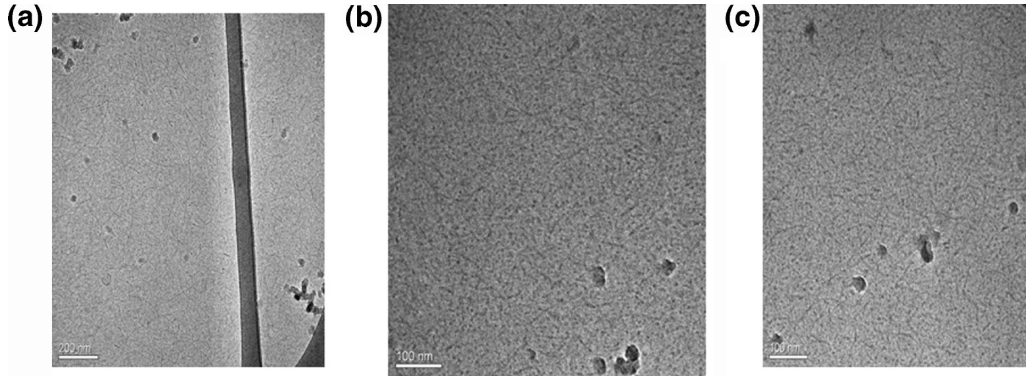

Figure 6. Cryo-TEM images of the spherical and thread-like micelles at C_o = 0.008 M in the 0.1 MCTAB/0.1 M KBr/octanol system at (a) bar = 200 and (b and c) = 100 nm.

Maxwell fluid-like behavior, again, is an indication of the presence of wormlike micelles in the solution.[28] With further increase in the concentration of C_8OH, the viscosity decreases and the characteristic Maxwell behavior disappears, indicating another structural transition which is in consonance with our viscosity data shown in Figure 1 (region III). The absence of a Maxwell type relaxation indicates that there are no entangled micelles. The fact that G' is higher than G'' indicates that elastic behavior dominates. Such relaxation is observed in concentrated vesicle phases where the ordering of vesicles leads to elastic gels.

It is relevant to note that at higher frequencies an elastic behavior was shown by the micelle phase ($G' > G''$), which switched to a viscous behavior ($G'' > G'$) at low frequencies (Figure 2a). The characteristic relaxation time, τ, of these viscoelastic samples, which is calculated as $1/\omega c$, where ωc is

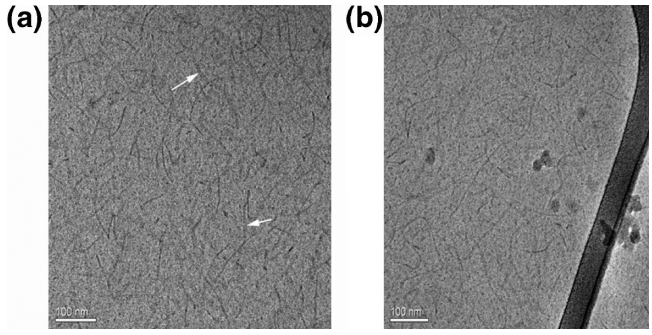

Figure 7. (a and b) Cryo-TEM images of wormlike micelles (arrow A) and ribbons (arrow B) at $C_o = 0.016$ M in the 0.1 MCTAB/0.1 M KBr/octanol system at bar = 100 nm.

the frequency at which G' and G'' cross, is found to increase and then decreases with an increase in the concentration of octanol.[32] The variation of G' and G'' is typical of gel phases arising from closely packed vesicles.

Figure 3 shows the effect of temperature on the oscillatory shear behavior of the sample in region II (Figure 1). It is observed that τ and η_0 decrease with an increase in temperature. Such decreases in η_0 and τ with temperature are expected for wormlike micelles—they result because of an exponential decrease in the micelle contour length with an increase in temperature.[6] This was further confirmed from the data given in Figure 2(a). It has been found that the Maxwell model fits the data reasonably well.

Vesicular dispersion is expected to be dilute in this phase, and therefore a nearly Newtonian behavior without much variation in viscosity is observed. Also, G'' is seen as higher than the G' in the whole experimental range of frequencies indicating the viscous nature of the sample. The increase in phase angle (δ)[43] from 56 to 77° (at a given frequency) for $C_o = 0.025$ M and $C_o = 0.035$ M, respectively, confirms the change of microstructure of the fluids, i.e., viscoelastic to viscous with increasing C_o. The low-phase angle value, $C_o = 0.025$ M, possibly indicates the coexistence of wormlike micelles and vesicles in the turbid phase (region III). The sharp decrease in viscosity may be due to the formation of vesicles.[28,33] The phase angle is related to the relative contribution of viscous and elastic components to the shear

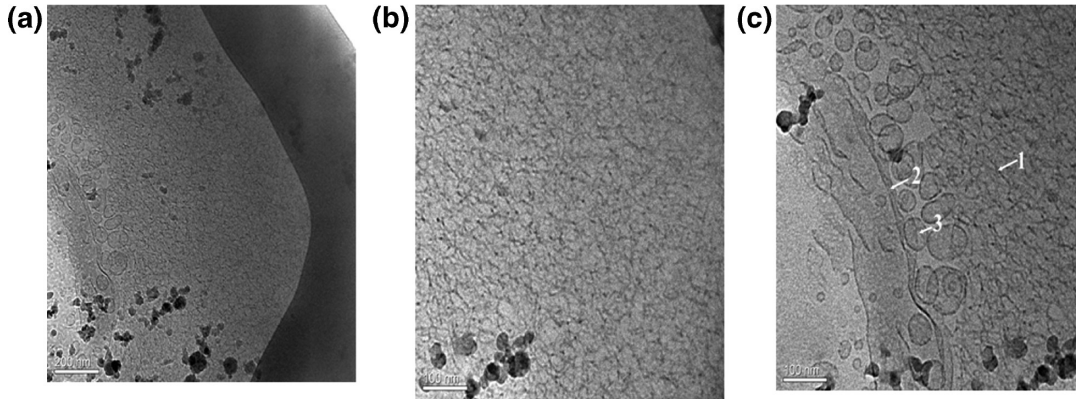

Figure 8. Micrographs obtained by cryo-transmission electron microscopy of samples located above the peak viscosity region $C_o = 0.025$ M at (a) bar = 200 and (b and c) 100 nm. The coexistence of threadlike micelles (arrow-1), bilayers (membrane sheets, arrow-2), and vesicles (arrow-3) can be seen here.

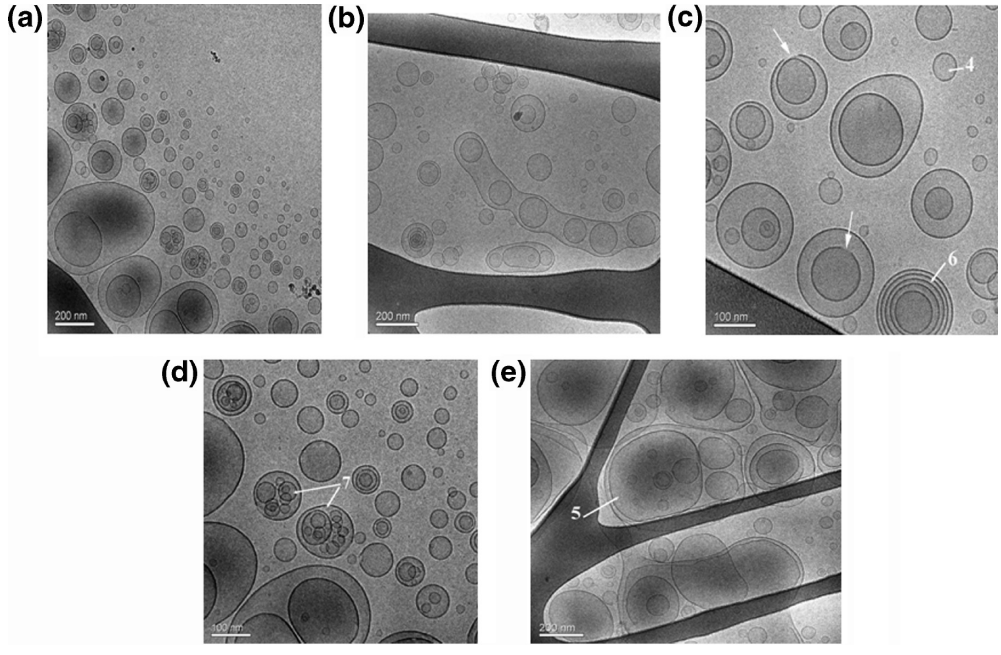

Figure 9. Cryo-TEM images of the 0.1 M CTAB/0.1 M KBr/octanol vesicle phase at $C_o = 0.035$ M at (a–c) bar = 200 and (d and e) = 100 nm. The unilamellar vesicles (arrow-4), multilamellar vesicles (arrow-6), and oligovesicular vesicle (arrows 5 and 7) were found in this region.

modulus. A phase angle greater than 45° indicates that viscous behavior dominates over the elastic behavior. As the phase angle approaches 90° the behavior becomes completely viscous. In the present study, an increase of phase angle indicates transition from the viscoelastic micelle phase to dilute vesicles (viscous). Thus, for a 0.1 M CTAB/0.1 M KBr/C_8OH micelle system, the sharp increase in viscosity begins at C_o= 0.008 M and leads to a maximum at C_o= 0.016 M extended up to C_o = 0.020, and then viscosity starts decreasing (region III). In region IV, an unusual increase in viscosity was noted with temperature. The data again demonstrate the onset of the transition which is dependent on the temperature indicating the presence of various types of vesicular structures (open, unilamellar, double lamellar).[29]

Dynamic light scattering (DLS) results [Figure 4 (a and b)] were very much complementary to the viscosity data shown in Figure 1 (region I). The temperature effect was studied for the chosen samples, from region I and from region IV (Figure 5 (a and b)). It is observed that the average hydrodynamic diameter, Z_{av}, increases with [C_8OH], indicating the presence of grown micelles present in region I. An interesting feature is observed in the DLS data shown in Figure 5. The sample from region I showed a decreased Z_{av} (Figure 5(b)) with temperature, whereas Z_{av} was found to increase for the sample from region IV. This again corroborates the viscosity and rheology results.

Figure 6(a−c) shows the cryogenic transmission electron microscopy cryo-TEM images of 0.1 M CTAB/0.1 M KBr/ 0.008 M octanol at 25 °C where we can observe the coexistence of spherical and wormlike micelles (region I). The formation of wormlike micelles is more pronounced at still higher concentration of octanol (Figure 7 (a and b)). These wormlike micelles impart high viscosity to the system, and the solution becomes viscoelastic as observed in region II of Figure 1 and by rheological study (Figure 2).

The cryo-TEM images of the micelle phase after the peak viscosity C_o > 0.016 M have been given in Figure 8(a−c), where we can observe the octanol-induced transition of wormlike micelles to the vesicle phase with a resultant drop in viscosity of the system. The coexistence of wormlike micelles (arrow-1), bilayers (membrane sheets, arrow-2), and vesicles (arrow-3) is also noticed in this region (region III). This observation is found to be in good agreement with the phase angle obtained for this region.

Cryo-TEM micrographs of the system at region IV (C_o > 0.025 M) give rise to the vesicle phase. It was observed that spontaneous formation of the vesicular phase depends on C_o, and it includes a wide size range. A wide spectrum of structures is illustrated in the images (Figure 9). Analyses of the micrographs show the complexity of the investigated mixed micelle system, including polydispersed vesicles with respect to size and shapes, with diameters in the range from d = 50 nm to d = 500 nm. The unilamellar vesicles (arrow-4), multilamellar vesicles (arrow-6), and oligovesicular vesicle (arrows 5 and 7) were found in this region. The values of the vesicular size obtained in the micrographs were in agreement with those obtained by other authors who investigated similar mixed micelle systems.[44,45]

Conclusions

We have demonstrated various microstructural transitions in a simple cationic micelle system. The system shows the transformation of a low viscous solution to a viscoelastic fluid followed by the formation of a turbid solution. The C_8OH was found to be a potential candidate to induce a rich variety of microstructures, which were found to be thermo reversible in nature. The DLS analyses at various temperatures of these aggregates were found to be complementary to viscosity and rheology studies. Spontaneous formation of unilamellar, multilamellar, and oligovesicles in the C_o range of 0.025−0.035 M and wormlike micelles in the C_o range of 0.008−0.016 M were thus confirmed by cryo-TEM studies.

Acknowledgment. The research support from UGC-DAE-CSR, Kalpakkam CRS-K-0/5/20, is gratefully acknowledged.

References and Notes

(1) Bijma, K.; Engberts, J. B. F. N. *Langmuir* **1997**, *13*, 4843–4849.
(2) Minkenberg, C. B.; Florusse, L.; Eelkema, R.; Koper, G. J. M.; vanEsch, J. V. *J. Am. Chem. Soc.* **2009**, *11*, 11274–11275.
(3) Vlachy, N.; Renoncourt, A.; Drechsler, M.; Verbavatz, J. M.; Touraud, D.; Kunz, W. *J. Colloid Interface Sci.* **2008**, *320*, 360.
(4) Chandler, D. *Nature* **2005**, *437*, 640–646.
(5) Segota, S.; Tezak, D. *Adv. Colloid Interface Sci.* **2006**, *121*, 51.
(6) Cates, M. E.; Candau, S. J. *J. Phys.: Condens. Matter* **1990**, *2*, 6869.
(7) Lin, Z.; Cai, J. J.; Scriven, L. E.; Davis, H. T. *J. Phys. Chem.* **1994**, *98*, 5984.
(8) Kern, F.; Lequeux, F.; Zana, R.; Candau, S. J. *Langmuir* **1994**, *10*, 1714.
(9) Ikeda, S.; Ozeki, S.; Tsunoda, M. *J. Colloid Interface Sci.* **1980**, *73*, 27.
(10) Rehage, H.; Hoffman, H. *Mol. Phys.* **1991**, *74*, 933.
(11) Aswal, V. K.; Goyal, P. S. *Phys. Rev.* **2000**, *61*, 2947.
(12) Weican, Z.; Ganzuo, L.; Jianhai, M.; Qiang, S.; Liqiang, Z.; Haojun, L.; Wu, Chi. *Chin. Sci. Bull.* **2000**, *45*, 1854.
(13) Wang, J. *Curr. Opin. Colloid Interface Sci.* **2002**, *7*, 276–281.
(14) Kabir-ud-Din; Kumar, S.; Kirti; Goyal, P. S. *Langmuir* **1996**, *12*, 1490.
(15) David, S. L.; Kumar, S.; Kabir-ud-Din, *J. Chem. Eng. Data* **1997**, *42*, 198.
(16) Kabir-ud-Din; Bansal, D.; Kumar, S. *Langmuir* **1997**, *13*, 5071.
(17) Hirch, E.; Candau, S.; Zana, R. *J. Colloid Interface Sci.* **1984**, *97*, 318.
(18) Lianos, P.; Zana, R. *Chem. Phys. Lett.* **1980**, *72*, 171.
(19) Kumar, S.; Khan, Z. A.; Kabir-ud-Din, *J. Surfactants Deterg.* **2002**, *5*, 55.
(20) Desai, A.; Varade, D.; Mata, J.; Aswal, V.; Bahadur, P. *Colloid Surf., A* **2005**, *259*, 111.
(21) Cappelaere, E.; Cressely, R. *Rheol. Acta* **2000**, *39*, 346.
(22) Khatory, A.; Kern, F.; Lequeux, F.; Appell, J.; Porte, G.; Morie, N. *Langmuir* **1993**, *9*, 933.
(23) Xia, G.; Hua, Li.; Zhang, F.; Zheng, S.; Guoa, R. *J. Colloid Interface Sci.* **2008**, *324*, 185.
(24) Akatsukaa, H.; Yamamotoa, M.; Oharaa, Y.; Otsubob, Y. *Colloids Surf., A* **2008**, *326*, 169.
(25) Patravale, V. B.; Mandawgade, S. D. *J. Cosmet. Sci.* **2008**, *30*, 19.
(26) Milchev, A. *Surf. Sci. Ser.* **2000**, *89*, 509–533.
(27) Ishiyama, N.; Hill, C. M.; bates, I.R. ; Haranz, G. *Chem. Phys. Lipids* **2002**, *114* (1), 103–11.
(28) Davies, T. S.; Ketner, A. M.; Raghavan, S. R. *J. Am. Chem. Soc.* **2006**, *128*, 6669.
(29) Danino, D.; Talmon, Y.; Zana, R. *Langmuir* **1995**, *11*, 1448–1456.
(30) Kumar, S.; Sharma, D.; Ghosh, G.; Kabir-ud-Din, *Langmuir* **2005**, *21*, 9446–9450.
(31) Sudheesh, P.; Nair, S. M.; Sreejith, L. *Asian J. Appl. Sci.* **2008**, *1*, 246.
(32) Sudheesh, P.; George, J.; Sajeev, M. S.; Sreejith, L. *J. Surfactants Deterg.* **2009**, *12*, 219–224.
(33) Hassan, P. A.; Valaulikar, B. S.; Manohar, C.; Kern, F.; Bourdieu, L.; Candau, S. J. *Langmuir* **1996**, *12*, 4350.
(34) Brown, J. C.; Pusey, P. N.; Dietz, R. *J. Chem. Phys.* **1975**, *62*, 1136.
(35) Bellare, J. R.; Davis, H. T.; Scriven, L. E.; Talmon, Y. *J. Electron Microsc. Tech.* **1988**, *10*, 87.
(36) Kohler, H. -H.; Strnad, J. *J. Phys. Chem.* **1990**, *94*, 7628.
(37) Mukerjee, P. In *Solution Chemistry of Surfactants*; Mittal, K. L., Ed; Plenum press: New York, 1979; p 153.
(38) Hoffmann, H. *Adv. Colloid Interface Sci.* **1990**, *32*, 123–150.
(39) Kaler, E. W.; Murthy, A. K.; Rodriguez, B. E.; Zasadzinski, J. A. N. *Science* **1989**, *245*, 1371–1374.

(40) Kalur, G. C.; Frounfelker, B. D.; Cipriano, B. H.; Norman, A. I.; Raghavan, S. R. *Langmuir* **2005**, *21*, 10998–11004.

(41) Acharya, D. P.; Kunieda, H. *Adv. Colloid Interface Sci.* **2006**, *123*, 401.

(42) Hassan, P. A.; Narayanan, J.; Manohar, C. *Curr. Sci.* **2001**, *80*, 980.

(43) Hassan, P. A.; Bhattacharya, K.; Kulshreshtha, S. K.; Raghavan, S.R. *J. Phys. Chem. B* **2005**, *109*, 8744.

(44) Viseu, M. I.; Edwards, K.; Campos, C. S.; Costa, S. M. B. *Langmuir* **2000**, *16*, 2105.

(45) Khan, A.; Regev, O. *Prog. Colloid Polym. Sci.* **1994**, *97*, 146.

JP1043255